1914

Trigonal prismatic versus octahedral coordination geometry of transition metal dithiolates: Comparison between saturated and unsaturated early transition metal tris(1,2-dithiolate) complexes

Joel L. Martin[1] and Josef Takats[2]

Department of Chemistry, University of Alberta, Edmonton, Alta., Canada T6G 2G2

Received February 20, 1989

This paper is dedicated to Professor Ronald J. Gillespie on the occasion of his 65th birthday

Joel L. Martin and Josef Takats. Can. J. Chem. **67**, 1914 (1989).

Reaction of a stoichiometric amount of $H_2edt/NaHedt$ (edt = ethane-1,2-dithiolate) with the appropriate metal amide, followed by cation exchange, gave the complexes $[NEt_4]_2[M(edt)_3]$ (M = Ti, **1**; Hf, **2**) and $[AsPh_4]$ $[Nb(edt)_3]\cdot CH_3CN$, **3**. The structure of **3** has been determined crystallographically (space group; cell dimensions; Z; unique data ($I \geq 3\sigma$ (I); R/R_w): $P\bar{1}$; $a = 9.095(1)$, $b = 14.609(3)$, $c = 15.639(3)$ Å and $\alpha = 60.09(2)$, $\beta = 80.07(3)$, $\gamma = 89.89(2)°$; $z = 2$; 1488; 4.3/4.5. The coordination geometry of **3** is severely distorted from the trigonal prismatic (TP) structure found in the analogous $Nb(1,2-S_2C_6H_4)_3^-$, which contains an unsaturated 1,2-dithiolate ligand system. The average twist angle between triangular faces is 33.3°. However, on the basis of VT ^1H NMR spectroscopy it is argued that the TP form is at most 9–10 kcal mol^{-1} less stable than the observed geometry. A comparison between the structures of tris-chelate complexes of the early transition metals containing saturated and unsaturated 1,2-dithiolates and related ligands is made, and the factors thought to be responsible for TP vs. octahedral geometry are reviewed and their relative importance assessed.

Key words: structure, trigonal prismatic, 1,2-dithiolate, early transition metals.

Joel L. Martin et Josef Takats. Can. J. Chem. **67**, 1914 (1989).

La réaction d'une quantité stoechiométrique de $H_2edt/NaHedt$ (edt = éthane-1,2-dithiolate) avec des amidures métalliques, suivie d'un échange de cation, fournit les complexes $[NEt_4]_2[Me(edt)_3]$ (M = Ti, **1**; Hf, **2**) et $[AsPh_4][Nb(edt)_3]\cdot CH_3CN$, **3**. On a déterminé la structure du composé **3** par diffraction des rayons-X. Les cristaux appartiennent au groupe d'espace $P\bar{1}$ avec $a = 9,095(1)$, $b = 14,609(3)$ et $c = 15,639(3)$ Å et $\alpha = 60.09(2)$, $\beta = 80,07(3)$ et $\gamma = 89,89(2)°$ et $Z = 2$; on a affiné la structure jusqu'à des valeurs respectives de R et R_w de 0,043 et 0,045 pour 1488 réflexions avec $I \geq 3\sigma(I)$. La géométrie de coordination du composé **3** est fortement deformée par rapport à la structure prismatique trigonale (PT) qui a été observée antérieurement avec l'analogue $Nb(1,2-S_2C_6H_4)_3^-$ qui contient un ligand 1,2-dithiolate insaturé. L'angle moyen de déviation entre les faces triangulaires est de 33,3°. Toutefois, sur la base de la RMN du ^1H à température variable, on suggère que la différence de stabilité entre la forme PT et la géométrie observée ne favorise cette dernière que par 9–10 kcal mol^{-1}. On a comparé les structures des complexes tris chélates des métaux de transition du début contenant des ligands 1,2-dithiolates saturés et insaturés ainsi que d'autres ligands apparentés; on passe en revue les facteurs que l'on croit responsable des structures PT vs. les géométries octaédriques et on évalue leurs importances relatives.

Mots clés : structure, prismatique trigonal, 1,2-dithiolate, métaux de transition du début.

[Traduit par la revue]

Introduction

The possibility of trigonal prismatic (TP) geometry in highly covalent d^0 transition metal complexes was predicted as early as 1932 by Hultgren (1), based on the concept of metal orbital hybridization presenting a more favorable bonding picture for TP than for octahedral geometry. This result has been corroborated by Hoffman *et al.* (2) on the basis of extended Hückel MO calculations.
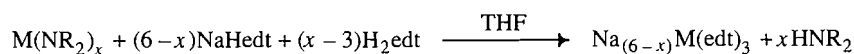
In 1965 the first observation of a discrete TP complex, $Re(1,2,-S_2C_2Ph_2)_3$ (3), rekindled interest in TP geometry and since then a host of factors, such as (a) ligand constraint (4, 5), (b) ligand field stabilization energy (2, 4, 6), (c) interdonor atom bonding (3, 7–9), (d) proper matching of ligand and metal orbital energies (1, 2, 10–12), (e) the symmetry of ligand π orbitals (2, 8, 13), and (f) the overall charge of the complex, have been suggested as important factors influencing the formation of TP, octahedral, or intermediate geometries. From experimental work of Holm and co-workers (4) and Eatough *et al.* (14) and theoretical work of Holm (4), Kepert (5), and Wentworth (6) it appears that the two most important factors involved are probably the ligand constraint (provided by cage type

---

[1]Present address: Phillips Petroleum Co., 96-G PRC, Bartlesville, OK 74004, U.S.A.

[2]Author to whom correspondence may be addressed.

ligands and (or) the "bite" distance of chelating ligands) and the ligand field stabilization energy in that order. However, the ordering of factors (c) through (f) is certainly still a subject of debate. Indeed any attempts to assess the importance of subtle electronic factors in favoring TP geometry must carefully avoid the problems of ligand constraint and ligand field stabilization energy. The studies that will be considered here were directed at understanding the geometry of transition metal complexes containing unsaturated 1,2-dithiols and attempted to avoid the complications of the two overriding factors mentioned above.
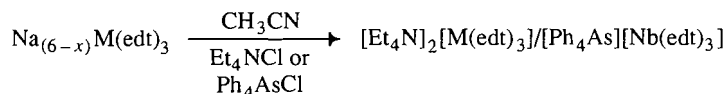
The synthesis of early transition metal complexes of benzene 1,2-dithiol (15) provided the unique opportunity to study an isoelectronic series of complexes: $Mo(bdt)_3$, $Nb(bdt)_3^-$, and $Zr(bdt)_3^{2-}$ (btd = 1,2-benzenedithiolate). Although the decreasing stability of TP geometry in the order Mo > Nb > Zr suggested to Cowie and Bennett (11) that the proper matching of metal d-orbital and ligand orbital energies was an important condition for TP geometry, the study was not conclusive because the change in overall charge of the complexes should also favor the observed trend. To confirm the hypothesis of Cowie and Bennett, we undertook structural analysis of $Ta(bdt)_3^-$ and $Sb(bdt)_3^-$ complexes, which strongly resemble the Nb complex in metal size and also have the same charge (12, 16). The increasing distortion away from TP geometry in the order Nb < Ta < Sb provides substantial evidence that the stability of TP

$$M(NR_2)_x + (6-x)NaHedt + (x-3)H_2edt \xrightarrow{THF} Na_{(6-x)}M(edt)_3 + xHNR_2$$

M = Ti and Hf, x = 4; Nb, x = 5

$$Na_{(6-x)}M(edt)_3 \xrightarrow[\substack{Et_4NCl \text{ or} \\ Ph_4AsCl}]{CH_3CN} [Et_4N]_2[M(edt)_3]/[Ph_4As][Nb(edt)_3]$$

M = Ti (1), Hf (2), Nb (3)

SCHEME 1

geometry hinges upon the availability of metal d orbitals of appropriate energy. Also, the study of the entire series of benzene-1,2-dithiolate complexes, in our mind, has cast serious doubt about the importance of interligand donor atom bonding in this regard.

However, an interesting question that remains is whether π bonding or σ bonding, as originally suggested by Hultgren (1) and later revived (10), is the factor that favors TP geometry. A possible approach to this question is to compare the behavior of analogous complexes containing unsaturated and saturated 1,2-dithiols, since the σ/π bonding capabilities of these ligand systems are expected to be different.

In this paper we present our synthesis of $M(edt)_3{}^{n-}$ (edta = ethane-1,2-dithiolate; M = Ti, Hf, n = 2; M = Nb, n = 1) complexes, describe the solid state structure of the niobium complex (tetraphenylarsonium salt), and comment on the relevance of these complexes to the question of TP vs. TAP coordination geometry in transition metal dithiolates. Since our initial disclosures (17), other groups have extensively investigated the chemistry and structure of transition metal complexes of ethane-1,2-dithiol (18–21). The synthesis and structure of $[NEt_4]_2[Ti(edt)_3]$ and $[NEt_4][Nb(edt)_3]$ have been reported by Holm and co-workers (20) and Tatsumi, Nakamura, et al. (21a), respectively.

Results

Synthesis and spectroscopic properties

As reported previously for the synthesis of the analogous benzene-1,2-dithiolate complexes (15), the reaction of the appropriate transition metal amide with $H_2edt/Hedt^-$, according to the stoichiometry shown in Scheme 1, gave the corresponding tris(ethane-1,2-dithiolate) complexes in moderate yield. The Ti and Nb (and Ta) complexes were also obtained from the reaction of the appropriate metal halide with Na_2edt and Li_2edt respectively, in the required 1:3 stoichiometric ratio (20, 21). It is not known whether the Hf complex also obtains from this simplified procedure.

The complexes reported are well-behaved, crystalline solids (1 and 3 red, 2 almost colorless), but are somewhat more unstable toward hydrolysis than the corresponding benzene-1,2-dithiolate compounds. Solutions of both types of compounds are sensitive to moisture carried in the air. Under inert atmosphere, complexes 1–3 are stable in CH_3CN but, like the corresponding benzene-1,2-dithiolate complexes, the Ti and Hf derivatives decompose in CH_2Cl_2. Stability in the solid state ranges from the readily hydrolyzed Hf compound to the reasonably unreactive Ti and to the stable Nb complex. However, we note that Tatsumi, Nakamura, et al. (21b) report an interesting rearrangement of the latter compound via C—S bond cleavage, a feature not observed with the analogous unsaturated dithiol complexes.

The infrared spectra of compounds 1 and 2 show two strong bands in the metal–sulfur stretching region (1, 355 and 322
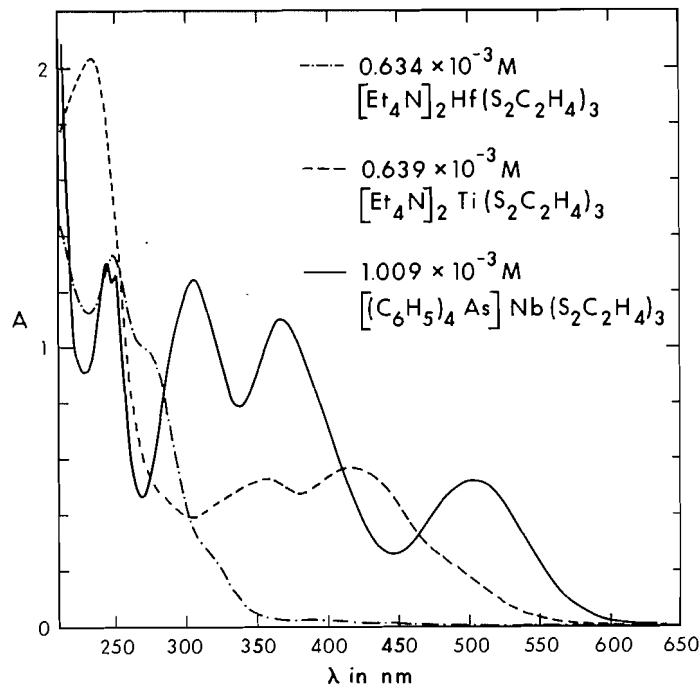

FIG. 1. Ultraviolet–visible absorption spectra of complexes 1–3 in acetonitrile.

cm^{-1}; 2, 297 and 268 cm^{-1}), and are tentatively thus assigned. The M–S stretching region for 3 is obscured by the tetraphenylarsonium ion bands, but Tatsumi, Nakamura, et al. (21a) report Nb–S and Ta–S stretching vibrations at 354(s), 338(s), 240(w) and 335(s), 318(s), 225(w) cm^{-1}, respectively. Once the difference in relative atomic masses between these metals is taken into account, the strength of the M–S stretch is Ti $\approx$ Hf < Ta $\approx$ Nb. The ^1H NMR spectra of the complexes at room temperature exhibit a sharp singlet for the methylene protons of the ligand. The position of the signal shifts to lower field in the order Hf, Ti, and Nb (δ: 2, 3.23; 1, 3.38; 3, 3.76 ppm), which is the same order as the stability sequence of the compounds. The cause of the strong coloration of the Ti and Nb complexes is evident from Fig. 1. Charge transfer transitions, which dominate the spectra, shift to higher energy in the order Nb < Ti < Hf. Systematic blue shift of all uv–visible absorption bands on going from $Nb(edt)_3{}^-$ to $Ta(edt)_3{}^-$ was also reported by Tatsumi, Nakamura, et al. (21). The dependence of the lowest energy maximum upon the metal is suggestive of LMCT character of the bands. A detailed assignment of the spectra cannot be made at this time, but it must be pointed out that the same type of metal dependence was observed in the benzene-1,2-dithiolate complexes.

The chemical reactivity, infrared spectra in the ν_{M-S} region, ^1H NMR spectra, and uv–visible spectra of the ethane-1,2-

TABLE 1. Selected distances (Å) and angles (deg) for [Ph₄As][Nb(1,2—$S_2C_2H_4)_3$]·CH_3CN, 3

Bond distances					
Nb—S(1)	2.438(3)	C(1)—S(1)	1.82(1)	C(1)—C(2)	1.50(2)
Nb—S(2)	2.432(3)	C(2)—S(2)	1.82(1)		
Nb—S(3)	2.422(4)	C(3)—S(3)	1.80(1)	C(3)—C(4)	1.49(2)
Nb—S(4)	2.435(3)	C(4)—S(4)	1.82(1)		
Nb—S(5)	2.419(3)	C(5)—S(5)	1.81(1)	C(5)—C(6)	1.52(2)
Nb—S(6)	2.438(4)	C(6)—S(6)	1.80(1)		

Intra- and inter-ligand S---S distances					
S(1)—S(2)	3.202(5)	S(1)—S(3)	3.305(5)	S(2)—S(4)	3.327(5)
S(3)—S(4)	3.178(5)	S(3)—S(5)	3.363(5)	S(4)—S(6)	3.374(5)
S(5)—S(6)	3.179(5)	S(5)—S(1)	3.287(5)	S(6)—S(2)	3.249(5)

Bond angles

"Bite"-angles		*trans*-angles	
S(1)—Nb—S(2)	82.2(1)	S(1)—Nb—S(4)	158.7(1)
S(3)—Nb—S(4)	81.7(1)	S(2)—Nb—S(5)	156.6(1)
S(5)—Nb—S(6)	81.8(1)	S(3)—Nb—S(6)	161.5(1)

Others

Nb—S(1)—C(1)	105.9(4)	S(1)—C(1)—C(2)	109.4(10)
Nb—S(2)—C(2)	105.2(4)	S(2)—C(2)—C(1)	109.6(10)
Nb—S(3)—C(3)	106.6(5)	S(3)—C(3)—C(4)	110.5(9)
Nb—S(4)—C(4)	105.8(4)	S(4)—C(4)—C(3)	109.6(10)
Nb—S(5)—C(5)	105.6(4)	S(5)—C(5)—C(6)	110.4(9)
Nb—S(6)—C(6)	107.9(5)	S(6)—C(6)—C(5)	110.1(10)

dithiolate complexes all show the trends expected for increased bond strength in the order Hf < Ti < Nb, just as in the benzene-1,2-dithiolate complexes. The rationale here, as before, is that the metal d orbitals are increasingly stabilized in the order Hf < Ti < Ta < Nb and as a result both σ and π donation from the ligand are enhanced. However, as yet no means other than X-ray crystallography has been developed that can answer questions regarding the exact geometry of the metal complexes. Accordingly, the single crystal X-ray structure of the Nb complex was determined.

Description of the structure of 3

A summary of pertinent distances and angles is presented in Table 1. Numbering of the Nb(edt)₃⁻ anion is evident from Fig. 2, which is a view down the approximate threefold axis of the complex anion. The contents of the unit cell are shown in Fig. 3 and establish that the crystal structure consists of well-separated ions and CH_3CN molecules, with no unusual interionic contacts. The disordered CH_3CN molecules are shown as five atoms, which was the model used to fit them. As may be expected for this type of disorder, the bond lengths and angles are slightly irregular and have large standard deviations. However, the C—C bond lengths, 1.35(5) and 1.40(4) Å, C≡N bond lengths, 1.17(5) and 1.18(5) Å, and C—C≡N bond angles, 174°(4) and 175°(4), are in agreement with accepted values. The geometry of the tetraphenylarsonium ion is in good agreement with previous determinations of this ion, with As—C bonds averaging 1.884(3) Å and C—As—C angles averaging 109.5(8)°.

Although there is no crystallographically imposed symmetry, it is clear from Fig. 2 that the complex anion is quite symmetrical. The six sulfur atoms are approximately equidistant from the
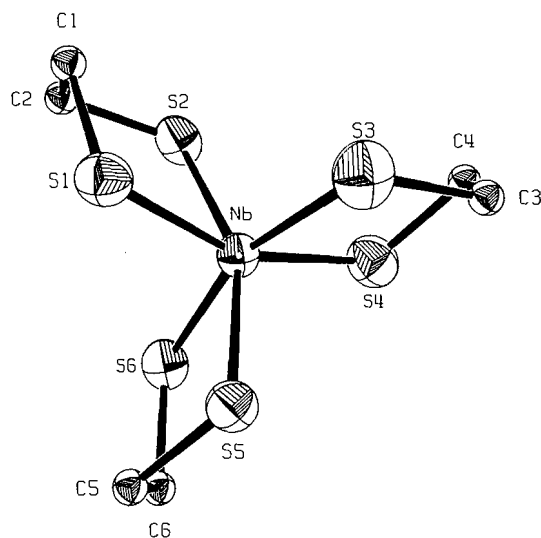

FIG. 2. A perspective view of the molecular structure of the complex anion, Nb(edt)₃⁻, in 3. The thermal vibrational ellipsoids for Nb and S atoms represent 50% probability, while the isotropic thermal parameters for C atoms have been reduced for clarity.

Nb center (Nb—S: 2.419(3)–2.438(3) Å, ave. 2.431(3) Å). The three five-membered chelate rings are disposed in a well-ordered propeller-like arrangement, each exhibiting the symmetric half-chain conformation. The angles also cover a fairly narrow range: S—Nb—S (bite), 81.7(1)–82.2(1)°; S—Nb—S (*trans*), 156.6(1)–161.5(1); ligand dihedral angles (SCCS), 59(1)° (S(1)—S(2)), 57(1)° (S(3)–S(4)), 55(1)° (S(5)–S(6)). The triangular faces at opposite ends of the complex anion
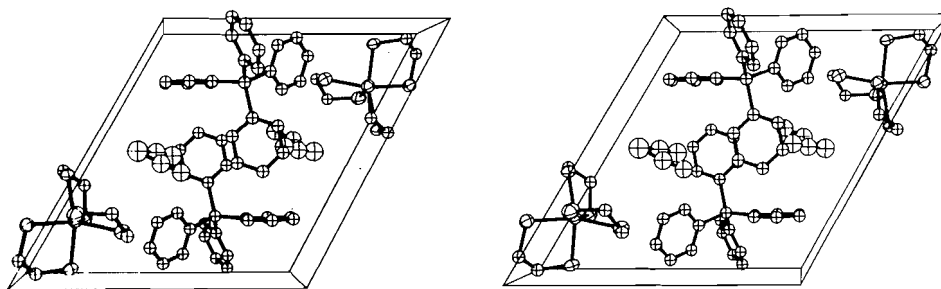
FIG. 3. A stereoview of the contents of the unit cell with b axis pointing to the right and c pointing upward.

TABLE 2. Selected distances (Å) and twist angle (deg) in tris(1,2-dithiolate) complexes

Compound	M—S	S—S(intra)	S—S(inter)	C—S	ϕ(ave)	ϕ(calcd.)[a]	Ref.
Nb(bdt)$_3^-$	2.441(11)	3.150(9)	3.23(5)	1.745(9)	0.7	48	10
Nb(edt)$_3^-$	2.431(3)	3.168(8)	3.32(2)	1.81(1)	33.3	49	This work
	2.434(1)	3.189(3)	3.30(4)	1.816(5)	30.5		19
Ti(edt)$_3^{2-}$	2.427(7)	3.213(3)		1.81(1)	38.0	51	18
Zr(bdt)$_3^{2-}$	2.543(10)	3.265(14)	3.58(14)	1.765(7)	37.0	46	10

[a]Obtained from ref. 4 and based on the normalized ligand bite distance (S—S(intra)/M—S).

(S(1,3,5) and S(2,4,6)) are tilted from being parallel by only 1°. The projected twist angles of the individual ligands (22), are $\phi_{1,2} = 32.6°$, $\phi_{3,4} = 33.3°$, and $\phi_{5,6} = 33.7°$ ($\phi_{ave} = 33.3°$) and indicate a coordination polyhedron intermediate between a trigonal prism and an octahedron. Thus the complex anion approximates D_3 molecular symmetry, the configuration shown in Fig. 2 is $\Delta(\lambda\lambda\lambda)$, and the unit cell of course contains the enantiomeric pair.

It is gratifying to note that the geometry of the complex anion in [NEt$_4$] [Nb(edt)$_3$] (21), 3', which contains a different counterion and crystallizes in a different space group, is nearly identical with the one found in 3. The pertinent values are: Nb—S$_{(ave)}$, 2.434(7) Å; S—Nb—S (bite), 81.58(4)–82.14(4)°; S—Nb—S (trans), 156.29(4)–157.55(4)°. The projected twist angles (ϕ) are: 31.4, 30.6, and 29.4° with the average value ($\phi_{ave} = 30.5°$) being only 2.8° different from that found in 3. The absolute configuration of 3' was determined as $\Lambda(\delta\delta\delta)$. Clearly the coordination geometry of the complex anion, Nb(edt)$_3^{2-}$, is determined mainly by electronic factors between the transition metal and the coordinated ethane-1,2-dithiolate; crystal packing forces can play but a minor role in this regard.

An immediate observation that can be made concerning the structure of 3 is that it has moved away from the TP geometry of the related Nb(bdt)$_3^-$ complex, which contains unsaturated 1,2-dithiolates, yet the stereochemistry of 3 is among the closest to the TP among complexes with non-dithiolene type ligands. To properly assess the importance and the degree of this distortion it is instructive to compare the structure of 3 with those of the closely related Ti(edt)$_3^{2-}$ and M(bdt)$_3^{n-}$ (M = Nb, $n = 1$; M = Zr, $n = 2$) complexes. The relevant distances and the projected twist angles are listed in Table 2.

The C—S bond distances in 3 are typical of carbon–sulfur single bonds involving sp^3 hybridized C and S atoms (predicted value 1.81, ref. 23). These distances are significantly longer than those in Nb(bdt)$_3^-$, even after corrected for the change from sp^3 to sp^2 carbon in the latter. It is then interesting that the change in ligand character is not accompanied by a change in Nb—S bond distances, which, if anything, are marginally shor-

ter in 3 featuring the saturated ethane-1,2-dithiolate ligand system. Thus the strength of the Nb—S interaction in the two complexes must be very similar even though the nature of the Nb—S interaction is different. A final note of interest is the very slight change in M—S distances on going to the Ti(edt)$_3^{2-}$ complex. The decrease is certainly less than anticipated from the change in ionic radii between two metal ions (0.03 Å) (24), and the longer than "predicted" distance is not inconsistent with the greater chemical reactivity of Ti(edt)$_3^{2-}$ compared to the Nb complex, and hence with the somewhat reduced Ti—S bond strength.

Reference to Table 2 shows that all the complexes listed present an average projected twist angle, ϕ_{ave}, that is smaller than the "corrected octahedral limit" imposed by the constraint of the ligand bite distance, thus indicating a real tendency of these systems to distort toward the TP geometry. The degree of distortion (measured by $\phi_{calc} - \phi_{ave}$) is Nb(bdt)$_3^-$ (47°) $\gg$ Nb(edt)$_3^-$ (17°) > Ti(edt)$_3^{2-}$ (13°) > Zr(bdt)$_3^{2-}$ (9°). Although it has been established that the ligand in Zr(bdt)$_3^{2-}$ is at the reduced dithiolate extreme (11), it is nevertheless noteworthy that the Ti(edt)$_3^{2-}$ and Nb(edt)$_3^-$ complexes, with saturated 1,2-dithiolate ligands, show a more severe twisting toward the prism. Clearly, unsaturation is not enough to stabilize the TP. The order of distortion toward the prismatic geometry Nb(edt)$_3^-$ > Ti(edt)$_3^{2-}$ > Zr(bdt)$_3^{2-}$ follows the progressive increase in d-orbital energies and further corroborates our contention that proper match between ligand and metal orbital energies is an important factor for prism stability. Yet the almost perfect TP geometry of Nb(bdt)$_3^-$ in contrast to the distorted geometry of Nb(edt)$_3^-$ also shows that unsaturated 1,2-dithiolates, and possibly related chelating ligands, have some additional property that further enhances the possibility for TP coordination geometry.

Varible temperature ^1H NMR study of 3

At ambient temperature the ^1H NMR spectrum of complex 3 shows a sharp singlet for the CH$_2$ hydrogen atoms.

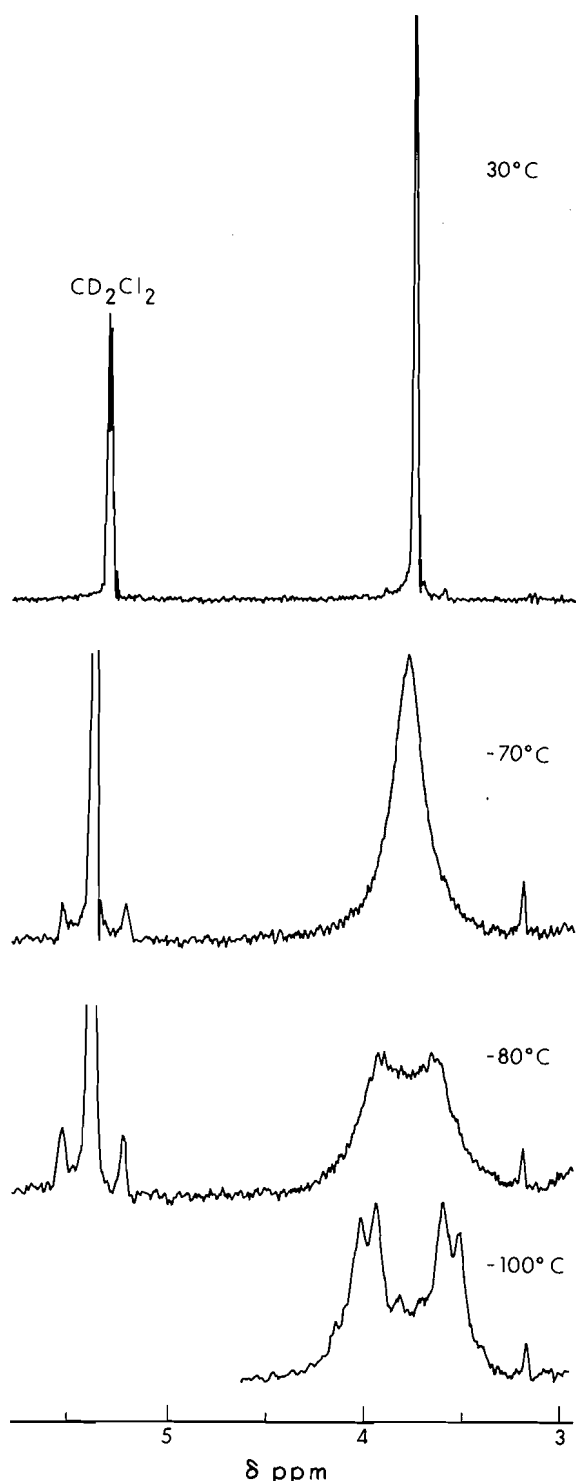From Fig. 2 it is evident that the methylene hydrogens of the

FIG. 4. Variable temperature ^{1}H NMR spectra of **3** in CD_2Cl_2.

ligands form two nonequivalent sets, H_{axial} and $H_{equatorial}$. As it is lucidly explained elsewhere (25), in the absence of racemization of such tris-chelate complexes the hydrogen atoms are inherently nonequivalent, even with rapid inversion of the puckered five-membered ring, and should give rise to an AA′BB′ pattern. Equilibration of the two types of hydrogen atoms and observation of a single resonance is only possible by operation of both processes.

Upon cooling a solution of **3** in CD_2Cl_2, the spectral changes shown in Fig. 4 are seen. By −103°C, a well-resolved AB

quartet is obtained, indicating stoppage of one of the previously mentioned processes. The $\Delta G^{\pm}$ associated with the process at −78°C is estimated as 9.2 kcal mol^{-1} (26). We have no direct proof that the observed fluxional behavior is intramolecular, but a dissociative process seems highly unlikely due to the reactivity of the free ligand with the solvent. Indeed the Ti and Hf complexes decompose in CH_2Cl_2. A spectrum obtained in the presence of excess of the free dithiol showed no evidence of ligand exchange.

Although it is not possible to delineate which of the two previously described processes has stopped at low temperature, should the racemization go via the trigonal twist type process, the barrier observed represents an upper limit for the stabilization of the twisted form over the TP geometry in this complex.

Discussion

As indicated in the Introduction, the major focus of this study was to compare the structure of early transition metal tris-chelate complexes containing the saturated ethane-1,2-dithiolate ligand with those of the analogous complexes with unsaturated benzene-1,2-dithiolate moieties, with a view to establishing the electronic factors responsible for changes in coordination geometry in the complexes.

To assess the anticipated bonding changes on going from the saturated to the unsaturated 1,2-dithiolate ligand, reference to the qualitative energy level diagram is made, Scheme 2. Ethane-1,2-dithiolate can act as a σ donor donating two electrons from a lone pair on each sulfur atom for a total of four σ electrons. In principle, it can also donate additional electrons to the metal from the remaining lone pairs on the sulfur atoms through the formation of π bonds, although the orientation of these lone pairs may not contribute to this very effectively (see Fig. 2). This situation has been considerably altered in the case of unsaturated 1,2-dithiolates. These ligands can still donate the same number of electrons through σ-bonding, but two of the remaining sulfur atom lone pairs have been delocalized over the ligand π framework. Two of these electrons have gone into a bonding orbital ($2\pi_v$) and have been somewhat stabilized, and the remaining two electrons have been placed into an antibonding orbital ($3\pi_v$) and have been destabilized. This π delocalization then has two effects. First, it reduces the effective charge on the sulfur atoms and therefore stabilizes the lone pairs and, second, it causes the ligand system to become a strong π donor due to the presence of the two antibonding π electrons. The whole ligand system is then a six-electron donor. From the above reasoning an important conclusion can be drawn regarding the relative behavior of saturated and unsaturated 1,2-dithiols, namely, that the former ligand system should be a better σ but poorer π donor than the latter. Also shown in the scheme is the oxidized, dithioketone formulation of the unsaturated ligand. Under this formulation, which is the more traditional view with these "dithiolene" type ligands (7, 8, 13), the ligand presents a low-lying symmetric π-acceptor orbital ($3\pi_v$) to the metal. Although the π-donor picture is more appropriate with the anionic complexes of the early transition metals since, as detailed elsewhere (11, 12, 15), these complexes contain the more reduced form of the unsaturated 1,2-dithiolates, it is clear that to achieve a unified picture for the possible importance of π bonding in stabilizing the TP geometry with different 1,2-unsaturated ligands the π-acceptor extreme will also have to be invoked.

Returning then to the structure of Nb(edt)$_3^-$, the distortion away from the TP geometry of the analogous Nb(bdt)$_3^-$ complex
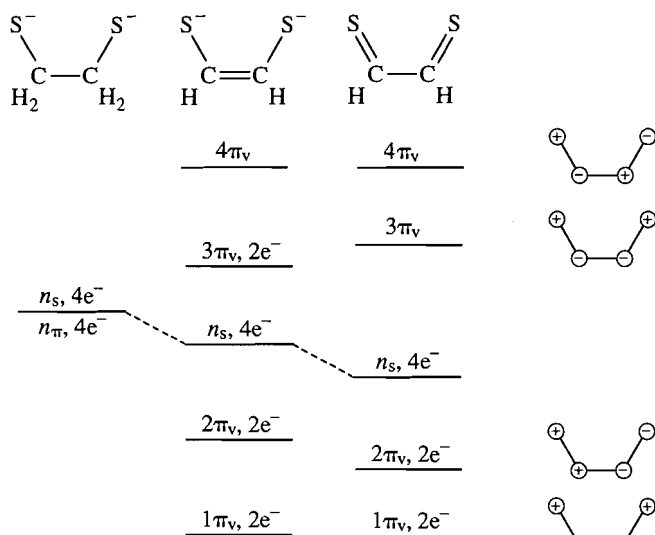
SCHEME 2
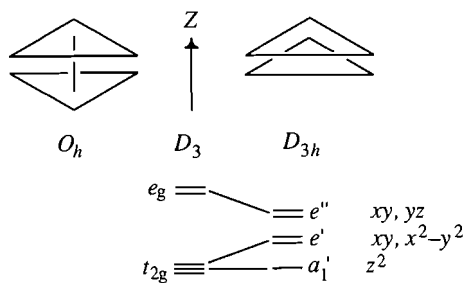
SCHEME 3

seems to imply that π bonding is responsible for, or at least contributes to, the stabilization of the TP geometry, since, according to the reasoning presented above, π bonding is expected to be less important with the saturated ethane-1,2-dithiolate than with the unsaturated benzene-1,2-dithiolate ligand system. Further support for this conclusion comes from a tris(1,2-dihydroxoethane) complex of tungsten, $W(OCH_2CH_2O)_3$ (27). This complex exhibits an average twist angle of 36.9°, once again intermediate between the TP and octahedral limits and in sharp contrast to the TP geometry observed for tris(9,10-phenanthrenequinone)molybdenum(0) (28).

To understand how π bonding can stabilize the TP geometry, let us consider the well-known level ordering of the predominantly metal d character orbitals in octahedral and TP ML_6 complexes, Scheme 3 (adapted from ref. 2), and the interaction of these orbitals with the unsaturated ligands in both π-acceptor and π-donor extremes. We recall that under D_{3h} symmetry (TP geometry) the $3\pi_v$ MOs of the ligands will give rise to two group molecular orbitals of a_2' and e' symmetries.

Let us first consider the ligands in their oxidized form. This situation implies metals in low oxidation states with their full complement of valence electrons in d-type orbitals. It is clear from the scheme that occupation of the high-lying e' orbitals, which will happen for any d^n electronic configuration with $n > 2$, will destablize the TP in favor of the octahedral geometry. However, the 1,2-dithioketone ligands have low-lying empty orbitals of e' symmetry (see above), which can effectively

stabilize the e' metal orbitals and hence lead to TP geometry. This is not a new result and had been considered by previous workers in the field (2, 8, 13). Nevertheless, it provides a natural link to other "even" type unsaturated ligands that present a symmetrical empty π-acceptor orbital to the central metal atom and properly account for the TP geometry observed in tris(buta-1,3-diene)molybdenum (29), tris(ortho-xylyl)tungsten (30), and tris(methylvinylketone)tungsten (31) (for the respective ligands see **a**, **b**, and **c**). Indeed recently Green, Mingos, et al.

a   b   c
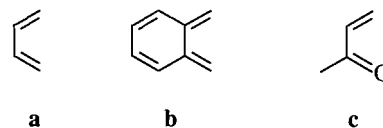
(32) have used molecular orbital calculations to support the importance of π back-bonding for the observed TP rather than octahedral geometry about the metal atom in tris(buta-1,3-diene)Mo/W. It is also worthy of note that the π-bonding model provides a rationale for the often observed folding of the ligand in TP complexes about the donor–donor axis, **d**, and, in a

d
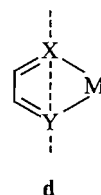
qualitative sense, for its extent. Clearly the all-carbon ligands (**a** and **b**) with no lone pair on the terminal atom(s) are the most oxidized of these unsaturated ligands and consequently elicit the largest amount of back-bonding from the metal to stabilize the e' orbital and achieve the TP geometry. This is accomplished by severe folding, to bring the $3\pi_v$ MO into maximal overlap with the metal e' orbital. Indeed all Mo—C bond distances in Mo(buta-1,3-diene)$_3$ were found equal (2.29(1) Å) (29). Replacing one CH_2 end group by an oxygen atom gives the methylvinylketone complex. Both σ donation from the oxygen lone pair and the more reduced nature of the ligand are expected to result in decreased π back-bonding and consequently to cause a smaller ligand folding. Reflecting these predictions, the terminal W—C and W—O distances (2.12(2) and 2.11(2) Å) are significantly shorter than the remaining W—C bonds (2.29(2) and 2.42(2) Å) (31). Continuing the trend toward more reduced ligands and less oxidized metal center, the situation with the unsaturated 1,2-dithiol type ligand with σ donation from two sulfur atoms, might have been expected to result in planar MS_2C_2 chelate rings. However, in most cases there is folding (11, 13). The folding of the planes within the same complex is sometimes irregular, and this is probably a consequence of crystal packing forces. Nevertheless we believe, as do Cowie and Bennett (11), that the major driving force for the ligand folding is to maximize the π bonding between $3\pi_v$ ligand molecular orbital and the metal e' (d_{xy}, $d_{x^2-y^2}$) orbitals. Ligand folding, but of an unusual type, has also been seen in the prismatic tris(9,10-phenanthrenequinone)molybdenum (28). Only one ligand is folded, the other two remain planar. However, the ligand exhibiting folding has longer C—C and Mo—O bond distances and shorter C=O bond lengths than the other two, closer to the oxidized form and hence in line with the folding arguments. We should like to close this section by mentioning that contrary to the TP geometry of the phenanthrenequinone complex, the structure of the related tetrachloro-1,2-benzoquinone derivative of chromium, Cr(1,2-

$O_2C_6Cl_4)_3$, is of the octahedral type (33). On the basis of structural parameters, Pierpont suggested that the metal center is best described as $Cr(O)$, d^6, with only very slight contribution from the ligand empty π-acceptor orbital in the bonding. Clearly the distortion away from TP finds explanation in the orbital picture shown in Scheme 3 and the d^6 electronic configuration of the metal.

The stability of TP geometry seems not to have been discussed as fully in terms of the π-donor model as the π-acceptor property of these ligands. Yet the two points of view must ultimately lead to the same conclusion since they represent two extremes of the electronic structure of the same ligand system. The physical reality, which depends on the nature of the metal and the ligand, must lie somewhere in between. Indeed it is easily appreciated that as the metal d orbitals and ligand π-acceptor levels approach one another in energy, the metal is gradually oxidized and the electrons are transferred into primarily ligand-based molecular orbitals. The acceptor oribitals are full and the π acceptor has been transformed into a π donor. Even though there is this transparent link between the two extremes, we wish to present a discussion of the π-donor model because, as stated before, the ligands in the early transition metal complexes are closer to the dithiolate limit. The analysis will attempt to clarily the behavior of the saturated 1,2-dithiolates and, as we shall see, it emphasizes different aspects of the M—S interaction.

Our analysis begins by considering the unsaturated ligand at the 1,2-ditholate extreme. Since the ligand is fully reduced, the accompanying metal ion is in the high, 6+, oxidation state. In this limit of highly ionic bonding, repulsion between ligand donor atoms dominates and the octahedral geometry is favored. This again is a well-known result (1, 2). As the ligand becomes a better π donor, the energy of the $3\pi_v$ donor molecular orbital approaches that of the metal d levels. Under D_{3h} symmetry (TP geometry) there can be effective overlap of the full ligand e' MOs and empty metal e' orbitals; electron density now flows from ligand to metal and results in strong, delocalized bonding with concomitant decrease in ligand donor atom repulsion and stabilization, or at least movement toward the TP geometry. We recognize that it is very difficult to dissociate the contribution from, and variation in, the M—S σ bonding from the overall molecular geometry, especially in view of the results of Hultgren (1) and Hoffman (2), which show that for d^0–d^2 electronic configurations M—S σ bonding alone could result in TP geometry. Nevertheless on the basis of the structural change between $Nb(bdt)_3^-$ (TP) and $Nb(edt)_3^-$ (distorted toward octahedral), we believe that the π component is a contributor to the overall stability of the TP. This energy contribution may be quite substantial, as seen with the strongly π-acceptor ligands (butadiene, methylvinylketone), or quite small, as evidenced by the small rearrangement barrier of the $Nb(edt)_3^-$ complex (*vide supra*).

It is especially evident from the above analysis that a major role of the highly delocalized π bonding and, of course, that of the primary σ component as well is to moderate interligand repulsion, otherwise the TP geometry would be unfavorable. Thus we would argue, along with Cowie and Bennett (11), against the still sometimes held belief that interligand S---S bonding is an important factor in stablizing the TP geometry. The postulate of interligand S---S bonding rests, to a large extent, upon the observation of constant prism dimensions in the series of compounds $Re(1,2,-S_2C_2Ph_2)_3$, $Mo(1,2-S_2C_2H_2)_3$,

and $V(1,2-S_2C_2Ph_2)_3$, despite the varying metal size (13). However, it can just as easily be argued that the observed interligand S---S distances in TP dithiolene complexes arise as a natural consequence of the TP geometry in complexes with M—S bond lengths on the order of 2.3–2.4 Å. The near constancy of M—S bond lengths in the previously mentioned V, Mo, and Re compounds may be a consequence of interligand donor atom repulsions tending to lengthen the M—S bonds in the smaller members rather than interligand S---S bonding determining the M—S bond length. There is some experimental support for the view that reducing interligand repulsion is important for the stability of the TP. In contrast to the distorted geometry of $Mo(mnt)_3^{2-}$ (mnt = $S_2C_2(CN)_2^{2-}$, maleonitriledithiolate) (34), the structure of $Mo(mnt)_2(dtc)^-$ (dtc = $S_2CNEt_2^-$, diethyldithiocarbamate) is TP (35).

To the best of our knowledge $Mo(mnt)_2(dtc)^-$ is the only compound containing the mnt^{2-} ligand that displays TP geometry and this may be due to an increased stabiliztion of the $3\pi_v$ orbital in this ligand and its attendant poor π-donor ability. While $Mo(mnt)_3^{2-}$ has a geometry distorted from TP, $Mo(qdt)_3^{2-}$ (qdt = quinoxaline-2,3-dithiolate, **e**) (36) and

e
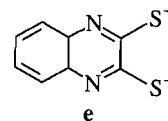
$Mo(S_2C_2(COOCH_3)_2)_3^{2-}$ (37) adopt TP geometry. The Mo—S distances in both compounds average 2.393 Å and are marginally longer than in the valence isoelectronic complex $Mo(mnt)_3^{2-}$ (2.324(8) Å). The corresponding interligand S---S distances of 3.141(7) and 3.18(6) Å are nearly the same as the 3.188 Å average for $Mo(mnt)_3^{2-}$, further calling into question the interligand sulfur bonding model.

In summary, trends in the uv–visible spectra, in the M–S stretching frequencies, in the reduction potentials, and in the structural parameters for early transition metal complexes with either benzene-1,2-dithiolate, ethane-1,2-dithiolate, or the recently reported propane-1,3-dithiolates (38) point to the fact that the metal d orbitals lie above the ligand π orbitals in energy. Moving to the right in the periodic table, the metal d orbitals are stabilized. This gives rise to π bonding first from the unsaturated dithiolates, which are stronger π donors. For high valence molybdenum and rhenium, the d orbitals appear to be sufficiently stable that TP geometry is even observed for the weaker π-donating, saturated ligands, as seen in $Mo(SCH_2CH_2SCH_2CH_2S)_2$ (39) and $Re[(SCH_2)_3CCH_3]_2^-$ (40), although constraint imposed by the tridentate ligand may also contribute to the observed geometry. Thus, while Gray's MO scheme provides a reasonable model for interpreting the uv–visible spectra, it appears to overestimate the stability of the metal d orbitals, for the earliest transition metals, with respect to the ligand $3\pi_v$ level. Consequently, it is necessary in that scheme to invoke bonding with the metal d_{z^2} orbital to arrive at the correct level ordering. We propose that the metal d_{z^2} orbital is largely nonbonding, therefore the occurrence of TP geometry for d^1 and d^2 complexes is not surprising and there are numerous examples (36, 37, 39–42). We are, therefore, drawn to the conclusion that overlap of the empty metal $d_{x^2-y^2}$ and d_{xy} orbitals with filled ligand π orbitals is more crucial to the appearance of TP geometry than interdonor atom bonding and is not limited to unsaturated 1,2-dithiolates. The charge of the complex ion, although of import, may also play a secondary role

as shown by the series of TP complexes $Mo(btd)_3$, $Mo(qdt)_3^{2-}$, and $Mo(S_2C_2(COOCH_3)_2)_3^{2-}$.

The final question to address is the importance of σ bonding relative to π bonding. The occurrence of TP geometry not only in dithiolates but also in tris(butadiene)molybdenum (29), tris-(ortho-xylyl)tungsten (30), tris(methylvinylketone)tungsten (31), $Tc(NHC_6H_4S)_3$ (42), $Mo(NHC_6H_4S)_3$, and tris(thioben-zoyldiazene)molybdenum (43) strongly implies that π bonding, if not an essential prerequisite, plays a significant role in stablizing this interesting coordintion geometry.

Experimental

All of the procedures and techniques used here have been described previously (15) except the modifications below. Reagent grade aceto-nitrile was dried by distillation first from P_2O_5 and then from CaH_2. Tetrahydrofuran was distilled from Na/K alloy. Commercially available ethane-1,2-dithiol was stirred at 0°C with a small amount of $LiAlH_4$ until the vigorous reaction subsided and then distilled and stored under nitrogen. Metal dialkylamides were prepared by published methods (44–47). Tetraethylammonium chloride was used as previously described (15).

Physical measurements

Visible and uv spectra were recorded at $\sim 10^{-3}$ M in CH_3CN on a Unicam SP 1700 spectrophotometer. ^1H NMR spectra were recorded on a Varian Associates A60 or HA-100 spectrometer. Infrared spectra were recorded as KBr pellets or mineral oil and Fluorolube mulls with CsI windows, for the low energy region, on a Perkin–Elmer 467 infrared spectrometer. All analyses were performed at the analytical facilities of the University of Alberta. The sample of the Hf complex used for analysis was weighed on a Cahn electrobalance in a dry box.

Preparation of [(C6H5)4As][Nb(1,2-S2C2H4)3]·CH3CN, 3

Sodium cyclopentadienide (2.70 mmol) in ~5 mL of THF was added to 0.60 mL (8.20 mmol) of ethane-1,2-dithiol in 50 mL of THF, resulting in the formation of a white precipitate. To this mixture 0.846 g (2.70 mmol) of pentakis(dimethylamido)niobium(V) was added in 20 mL of THF and the reaction mixture rapidly turned dark red. The mixture was stirred for ~20 h after which time a dark red precipitate was observed. Solid tetraphenylarsonium chloride (1.13 g, 2.70 mmol) was added and, after stirring 1 h, the solvent was stripped off under vacuum and replaced by 100 mL of CH_3CN. After stirring for ~20 h, most of the solid still had not dissolved so the mixture was heated to boiling and filtered hot. By cooling the filtrate overnight at $\sim -10°C$, dark red crystals were obtained. After filtration and vacuum drying, 0.60 g (30% yield) of product was obtained. Treating the residue above with an additional 100 mL of CH_3CN produced 0.28 g of product for a total of 41% yield. The two crude products were recrystallized from 100 mL of boiling CH_3CN and, after filtration and cooling, 0.60 g of product was obtained, mp 131–138°C (dec.) uncorrected; uv–visible λ_{max} (nm) (10^{-3} ε, M^{-1} cm^{-1}): 245(12.6), 251(12.2), 307(12.1), 369(10.7), 504(5.1); ^1H NMR (CD_2Cl_2) δ: 7.5–8.0 (complex multi-plet, 20H, Ph), 3.75 (s, 6H, CH_2) 1.96 (singlet, 3H, CH_3CN). Anal. calcd. for $C_{32}H_{35}AsNS_6Nb$: C 48.41, H 4.44, N 1.76, S 24.24; found: C 48.45, 48.25; H 4.53, 4.48; N 1.80, 1.71; S 23.65, 23.56.

Preparation of [(C2H5)4N]2[Ti(1,2-S2C2H4)3], 1

Sodium cyclopentadienide (0.68 g, 7.80 mmol) in 20 mL of THF was added to 0.98 mL (11.6 mmol) of ethane-1,2-dithiol in 30 mL of THF. Tetrakis(diethylamido)titanium(IV) (3.68 mmol) in 20 mL of THF was added next, resulting in a brown solution that gradually turned orange and finally red. The sodium salt of the Ti complex is soluble, in contrast to Nb. After stirring for ~18 h, 25.8 mL of a 0.272 M solution of tetraethylammonium chloride in CH_3CN was added, resulting in formation of an orange precipitate. The solvent was stripped off under vacuum and replaced by 50 mL of CH_3CN. After stirring ~½ h the mixture was filtered to give a red solution. By alternately cooling and concentrating the solution, the product was

TABLE 3. Crystal data for [Ph4As][Nb(edt)3]·CH3CN, 3

Parameter	Value
Molecular formula	$C_{32}H_{35}AsNS_6Nb$
Molecular weight	793.85
a, Å	9.095(1)
b, Å	14.609(3)
c, Å	15.639(3)
α, deg	60.09(2)
β, deg	80.07(3)
γ, deg	89.89(2)
V, Å^3	1766(1)
Z	2
Space group	$P\bar{1}$
$\rho_c(\rho_o)$, g cm^{-3}	1.495(1.49)
Crystal size, mm^a	0.19 × 0.16 × 0.15
	0.21 × 0.10 × 0.09
μ(MoKα), cm^{-1}	15.97
Transmission factors	0.89 × 0.92
Scan method	θ–2θ
Scan speed, deg min^{-1}	1.0
Scan width, deg^b	2.0 + $\Delta 2\theta$
2θ range, deg	36
Number of measured reflections	2223
Number of observed reflections $I \geq 3\sigma(I)$	1488
Number of variables	146
Goodness of fit (GOF)	1.6
Final R, R_w	0.043, 0.045

^{a}See text for explanation for using two crystals.
$^b\Delta 2\theta$ is a correction in the scan width for the dispersion of the $K_{\alpha 1}$–$K_{\alpha 2}$ doublet.

finally obtained as large dark-red crystals. However, on occasion a yellow decomposition product was observed in small quantities and was filtered off. The yield of dark-red crystals was 0.698 g, 34%; ir ν_{Ti-s}: 355 and 332 cm^{-1}; uv–visible λ_{max} (nm) (10^{-3} ε, M^{-1} cm^{-1}): 233(33.2), 357(9.0), 414(9.6); ^1H NMR (CD_3CN) δ: 3.38 (s, 6H, CH_2 anion), 3.30 (q, 16H, CH_2N), 1.24 (tt, 24H, CH_3N). Anal. calcd. for $C_{22}H_{52}NS_6Ti$: C 45.17, H 8.96, N 4.79, S 32.89; found: C 45.11, 45.28, H 8.91, 9,04; N 5.12; S 32.71, 31.97.

Preparation of [(C2H5)4N]2[Hf(1,2-S2C2H4)3], 2

This compound was prepared in the same way as the Ti compound above and was obtained as a single crystal ~1 cm long, yield 0.683 g, 23%. The product is almost colorless; ir ν_{Zr-s}: 297 and 268 cm^{-1}; uv–visible λ_{max} (nm) (10^{-3} ε, M^{-1} cm^{-1}): 249(20.4), 272 sh (15.1); ^1H NMR (CD_3CN) δ: 3.23 (s, 6H, CH_2 anion), 3.30 (q, 16H, CH_2N), 1.25 (tt, 24H, CH_3N). Anal. calcd. for $C_{22}H_{52}NS_6Hf$: C 36.93, H 7.32, N 3.91; found: C 36.64, 36.71; H 7.19, 7.25; N 3.88.

X-ray analysis of 3

Dark-red crystals of the compound were obtained by slow cooling of a saturated CH_3CN solution.

Details of the crystal data, intensity collection, and refinement are given in Table 3.

Weissenberg photographs using CuKα radiation and precession photographs using MoKα radiation revealed no systematic absences and $\bar{1}$ Laue symmetry. The intensity data were collected on a Picker FACS-1 four-circle automated diffractometer at ambient temperature using graphite monochromated MoKα radiation. Accurate cell dimensions were determined using 12 general reflections ($34° < 2\theta < 38°$). Intensity data were collected by the θ–2θ technique with background counts of 20 s at each end of the scan range. A set of three standard reflections was collected every 100 measurements, and an additional set of 10 reflections every 24 h, to test for crystal alignment and

TABLE 4. Fractional atomic coordinates and temperature factors for
$[Nb(edt)_3]^-$

Atom	x	y	z	$B_{eq},^a$ Å^2
Nb	0.1859(1)	0.09267(8)	0.23732(8)	3.07
As	0.8294(2)	0.5917(1)	0.2362(1)	3.36
S(1)	0.1429(4)	-0.0670(2)	0.2287(2)	4.46
S(2)	0.2788(4)	0.1691(3)	0.0576(2)	4.28
S(3)	-0.0850(4)	0.0873(3)	0.2736(3)	5.07
S(4)	0.1684(4)	0.2745(2)	0.2010(3)	4.58
S(5)	0.1732(4)	-0.0283(3)	0.4150(2)	4.25
S(6)	0.4495(4)	0.1159(3)	0.2410(2)	4.17
C(1)	0.170(2)	-0.024(1)	0.096(1)	6.12
C(2)	0.305(2)	0.056(1)	0.039(1)	5.78
C(3)	-0.127(2)	0.206(1)	0.277(1)	5.58
C(4)	-0.026(2)	0.299(1)	0.193(1)	5.24
C(5)	0.365(2)	-0.057(1)	0.428(1)	5.00
C(6)	0.470(2)	0.044(1)	0.370(1)	5.68

^{a}These are "equivalent" isotropic thermal parameters calculated from the anisotropic temperature factors by the program SFLS5.

stability. Approximately halfway through the collection, the intensity of the standards fell of sharply. Another crystal was mounted and collection resumed; this time no significant intensity changes were observed. The data were corrected for Lorentz and polarization effects and by an empirical absorption correction. The redundant data between the two crystals were merged.

The structure was solved by a combination of Patterson and difference Fourier maps and refined (using two scale factors) by full-matrix least-squares methods; the function minimized was $\Sigma w(|F_o| - |F_c|)^2$. Various models were attempted to describe the disordered CH_3CN molecule. Finally, use of a five-atom model, two acetonitriles with a common terminal carbon atom, seemed justified. Using occupancies of 0.45 and 0.55 for the two molecules, based upon the behavior of thermal parameters, reasonable bond distances were obtained by alternate refinement of the two molecules with all other parameters fixed. In the last two cycles of refinement the acetonitrile was not refined but the tetraphenylarsonium hydrogens were included as rigid bodies (C—H, 0.95°), also not refined. A final difference Fourier synthesis revealed peaks of 0.61, 0.56, and 0.47 e/Å^3 in the vicinity of the tetraphenylarsonium rigid bodies and a peak of 0.45 e/Å^3 near an acetonitrile carbon atom. All other features were less than 0.37 e/Å^3. The programs used in this study are those described previously (12).

Atomic coordinates and equivalent isotropic thermal parameters for the complex anion $Nb(edt)_3^{2-}$ are listed in Table 4. Anisotropic thermal parameters of the anion, atomic coordinates and thermal parameters for the rest of the complex, and structure factors are available as supplementary material in Tables S1–S3, respectively.[3]

Acknowledgement

1. R. HULTGREN. Phys. Rev. **40**, 891 (1932).
2. R. HOFFMAN, J. M. HOWELL, and A. R. ROSSI. J. Am. Chem. Soc. **98**, 2484 (1976).
3. R. EISENBERG and J. A. IBERS. J. Am. Chem. Soc. **87**, 3776 (1965).
4. E. LARSON, G. N. LA MAR, B. E. WAGNER, J. E. PARKS, and R. H. HOLM. Inorg. Chem. **11**, 2652 (1972).

[3]These tables may be purchased from the Depository of Unpublished Data, CISTI, National Research Council of Canada, Ottawa, Ont., Canada K1A 0S2.

5. D. L. KEPERT. Inorg. Chem. **11**, 1561 (1972); Inorganic stereochemistry. Springer-Verlag, Berlin. 1982.
6. R. A. D. WENTWORTH. Coord. Chem. Rev. **9**, 171 (1973).
7. G. N. SCHRAUZER and V. P. MAYWEG. J. Am. Chem. Soc. **88**, 3235 (1966).
8. E. I. STIEFEL, R. EISENBERG, R. C. ROSENBERG, and H. B. GRAY. J. Am. Chem. Soc. **88**, 2956 (1966).
9. A. AVDEEF and J. P. FACKLER, JR. Inorg. Chem. **14**, 2002 (1975).
10. R. HUISMAN, R. DEJONGE, C. HAAS, and F. JELLINEK. J. Solid State Chem. **3**, 56 (1971).
11. M. COWIE and M. J. BENNETT. Inorg. Chem. **15**, 1595 (1976); **15**, 1589 (1976); **15**, 1584 (1976).
12. J. L. MARTIN and J. TAKATS. Inorg. Chem. **14**, 1358 (1975).
13. R. EISENBERG. Prog. Inorg. Chem. **12**, 295 (1970).
14. D. J. EATOUGH, J. J. CHRISTENSEN, and R. M. IZATT. Chem. Rev. **74**, 351 (1974).
15. J. L. MARTIN and J. TAKATS. Inorg. Chem. **14**, 73 (1975).
16. J. L. MARTIN and J. TAKATS. Acta Crystallogr. Submitted.
17. J. L. MARTIN and J. TAKATS. 172nd ACS National Meeting, San Francisco, CA. 1976. Abstract INOR 181.
18. J. K. MONEY, J. C. HUFFMANN, and G. CHRISTOU. Inorg. Chem. **27**, 507 (1988).
19. W. TREMEL, M. KRIEGE, B. KREBS, and G. HENKEL. Inorg. Chem. **27**, 3886 (1988).
20. R. N. MUKHERJEE, CH. PULLA RAO, and R. H. HOLM. Inorg. Chem. **25**, 2979 (1986); **25**, 428 (1986).
21. K. TATSUMI, Y. SEKIGUCHI, A. NAKAMURA, R. E. CRAMER, and J. J. RUPP. (a) Angew. Chem. Int. Ed. Engl. **25**, 86 (1986); (b) J. Am. Chem. Soc. **108**, 1358 (1986).
22. K. R. DYMOCK and G. J. PALENIK. Inorg. Chem. **14**, 1220 (1975).
23. L. PAULING. The nature of the chemical bond. Cornell University Press, Ithaca, NY. 1966. p. 224.
24. R. D. SHANNON. Acta Crystallogr. Sect. A: Cryst. Phys. diffr. Theor. Gen. Crystallogr. **32**, 751 (1976).
25. T. G. APPLETON, J. R. HALL, and C. J. HAWKINS. Inorg. Chem. **9**, 1209 (1970); C. J. HAWKINS and J. A. PALMER. Coord. Chem. Rev. **44**, 1 (1982).
26. D. KOST, E. H. CARLSON, and M. REBAN. J. Chem. Soc. Chem. Commun. 656 (1971).
27. V. J. SCHERLE and F. A. SCHRÖDER. Acta Crystallogr. Sect B: Struct. Crystallogr. Cryst. Chem. **30**, 2772 (1974).
28. C. G. PIERPONT and R. M. BUCHANAN. J. Am. Chem. Soc. **97**, 4912 (1975).
29. P. S. SKELL and M. J. MCGLINCHEY. Angew. Chem. Inter. Ed. Engl. **14**, 195 (1975).
30. M. F. LAPPERT, C. L. RALSTON, B. W. SKELTON, and A. H. WHITE. J. Chem. Soc. Chem. Commun. 485 (1981).
31. R. E. MORIARTY, R. D. ERNST, and R. BAU. J. Chem. Soc. Chem. Commun. 1242 (1972).
32. J. C. GREEN, M. R. KELLY, P. D. GREBENIK, C. F. BRIANT, N. A. MCEVOY, and D. M. P. MINGOS. J. Organomet. Chem. **228**, 239 (1982).
33. C. G. PIERPONT and H. H. DOWNS. J. Am. Chem. Soc. **98**, 4834 (1976).
34. G. F. BROWN and E. I. STIEFEL. Inorg. Chem. **12**, 2140 (1973).
35. W. P. BOSMAN and A. NIEUWPOORT. Inorg. Chem. **15**, 775 (1975).
36. (a) S. BOYDE, C. D. GARNER, J. H. ENEMARK, and R. B. ORTEGA. Polyhedron, **5**, 377 (1986); (b) S. BOYDE, C. D. GARNER, J. H. ENEMARK, M. A. BRUCK, and J. G. KRISTOFZSKI. J. Chem. Soc. Dalton Trans. 2267 (1987).
37. M. DRAGANJAC and D. COUCOUVANIS. J. Am. Chem. Soc. **105**, 139 (1983).
38. K. TATSUMI, I. MATSUBARA, Y. SEKIGUCHI, A. NAKAMURA, and C. MEALLI. Inorg. Chem. **28**, 773 (1989).
39. J. HYDE, L. MAGIN, and J. ZUBIETA. J. Chem. Soc. Chem. Commun. 204 (1980).

40. P. J. Blower, J. R. Dilworth, J. P. Hutchinson, and J. Zubieta. Transition Met. Chem. **7**, 353 (1982).
41. S. F. Colmanet, G. A. Williams, and M. F. Mackay. J. Chem. Soc. Dalton Trans. 2305 (1987).
42. J. Baldes, J. Boas, J. Bonnyman, M. F. Mackay, and G. A. Williams. Aust. J. Chem. **35**, 2413 (1982).
43. J. R. Dilworth, J. Hyde, P. Lyford, P. Vella, K. Venkatasubraman, and J. A. Zubieta. Inorg. Chem. **18**, 268 (1979).
44. D. C. Bradley and I. M. Thomas. J. Chem. Soc. 3857 (1960).
45. D. C. Bradley and I. M. Thomas. Can. J. Chem. **40**, 449 (1962); **40**, 1355 (1962).
46. D. C. Bradley and M. H. Gitlitz. J. Chem. Soc. A, 980, (1969).
47. G. Chandra and M. F. Lappert. J. Chem. Soc. A, 1940 (1968).

This article has been cited by:

1. Saikat Bolar, Subhasis Shit, Naresh C. Murmu, Tapas Kuila. 2020. Doping-Assisted Phase Changing Effect on MoS 2 Towards Hydrogen Evolution Reaction in Acidic and Alkaline pH. *ChemElectroChem* **7**:1, 336-346. [Crossref]

2. Robert H. Morris. 2017. Six coordinate capped trigonal bipyramidal complexes. *Coordination Chemistry Reviews* **350**, 105-116. [Crossref]

3. K.C. Potgieter, T.I.A. Gerber, R. Betz, L. Rhyman, P. Ramasami. 2013. Structural and DFT/TD-DFT investigation of tris(bidentate) complexes of rhenium(III) synthesized from the cis-[ReO2]+ core and benzenethiol derivatives. *Polyhedron* **59**, 91-100. [Crossref]

4. Thomas Elder, Joseph J. Bozell, Diana Cedeno. 2013. The effect of axial ligand on the oxidation of syringyl alcohol by Co(salen) adducts. *Physical Chemistry Chemical Physics* **15**:19, 7328. [Crossref]

5. Raúl Colorado-Peralta, Mario Sanchez-Vazquez, Irán F. Hernández-Ahuactzi, Sonia A. Sánchez-Ruiz, Rosalinda Contreras, Angelina Flores-Parra, Silvia E. Castillo-Blum. 2012. Structural study of molybdenum(VI) complexes containing bidentate ligands: Synthesis, characterization and DFT calculations. *Polyhedron* **48**:1, 72-79. [Crossref]

6. Federica Maratini, Luciano Pandolfo, Silvia Rizzato, Alberto Albinati, Alfonso Venzo, Eugenio Tondello, Silvia Gross. 2011. A Tetranuclear Planar Hafnium Complex Containing O-Hf-S Moieties. *European Journal of Inorganic Chemistry* **2011**:22, 3281-3283. [Crossref]

7. Christian Schulze Isfort, Tania Pape, F. Ekkehardt Hahn. 2005. Synthesis and X-ray Molecular Structure of (PNP)2[MoIV(C6H4S2-1,2)3] Completing the Structural Characterization of the Series [Mo(C6H4S2-1,2)3]n- (n = 0, 1, 2). *European Journal of Inorganic Chemistry* **2005**:13, 2607-2611. [Crossref]

8. Remy van Gorkum, Francesco Buda, Huub Kooijman, Anthony L. Spek, Elisabeth Bouwman, Jan Reedijk. 2005. Trigonal-Prismatic vs. Octahedral Geometry for MnII Complexes with Innocent Didentate Ligands: A Subtle Difference as Shown by XRD and DFT on [Mn(acac)2(bpy)]. *European Journal of Inorganic Chemistry* **2005**:11, 2255-2261. [Crossref]

9. T. Waters, A.G. Wedd, M. Ziolek, I. Nowak. Niobium and Tantalum 241-312. [Crossref]

10. Richard D. Adams, O-Sung Kwon, Mark D. Smith. 2001. New evidence on the factors affecting bridging and semibridging character of carbonyl ligands. The structures of Mn 2 (CO) 7 (μ-SCH 2 CH 2 S) and its phosphine derivatives Mn 2 (CO) 7-X (PMe 2 Ph) X (μ-SCH 2 CH 2 S), × = 1,2. *Israel Journal of Chemistry* **41**:3, 197-206. [Crossref]

11. Subramanya Gupta Sreerama, Satyanarayan Pal, Samudranil Pal. 2001. A trigonal prismatic Mn(II) complex, [MnL(H2O)]2+, with bis(picolinylidenehydrazyl)(2-pyridyl)methane (L). Synthesis, structure and properties. *Inorganic Chemistry Communications* **4**:11, 656-660. [Crossref]

12. Martin Kaupp. 2001. Nicht-VSEPR-Strukturen und chemische Bindung in d0-Systemen. *Angewandte Chemie* **113**:19, 3642-3677. [Crossref]

13. Martin Kaupp. 2001. Nicht-VSEPR-Strukturen und chemische Bindung in d0-Systemen. *Angewandte Chemie* **113**:19, 3642-3677. [Crossref]

14. Shariff E Kabir, Caroline A Johns, K.M Abdul Malik, M.Abdul Mottalib, Edward Rosenberg. 2001. Reactivity of the unsaturated triosmium cluster [(μ-H)Os3(CO)8{Ph2PCH2P(Ph)C6H4}] with dithiols; X-ray structures of [Os3(CO)8(μ-SCH2CH2CH2S)(Ph2PCH2PPh2)]·1/2CH2Cl2 and [(μ-H)Os3(CO)7(μ3-η3-SCH2CH2CHS)(Ph2PCH2PPh2)]·1/2H2O. *Journal of Organometallic Chemistry* **625**:1, 112-120. [Crossref]

15. R.B. King. 2001. Chemical applications of topology and group theory. *Journal of Organometallic Chemistry* **623**:1-2, 95-100. [Crossref]

16. Khandakar M Hanif, Shariff E Kabir, M.Abdul Mottalib, Michael B Hursthouse, K.M.Abdul Malik, Edward Rosenberg. 2000. Dithiolate complexes of ruthenium and osmium: X-ray structures of [Ru2(CO)6(μ-SCH2CH2S)] and [{(μ-H)M3(CO)10)}2(μ-SCH2CH2CH2S)] (M=Ru, Os). *Polyhedron* **19**:9, 1073-1080. [Crossref]

17. Martin Kaupp. 1999. Im Niemandsland der Sechsfach-Koordination bei d0-Übergangsmetallkomplexen: Strukturvorhersagen für [WCl5CH3], [WCl4(CH3)2] und [WCl3(CH3)3]. *Angewandte Chemie* **111**:20, 3219-3221. [Crossref]

18. Martin Kaupp. 1999. Im Niemandsland der Sechsfach-Koordination bei d0-Übergangsmetallkomplexen: Strukturvorhersagen für [WCl5CH3], [WCl4(CH3)2] und [WCl3(CH3)3]. *Angewandte Chemie* **111**:20, 3219-3221. [Crossref]

19. Paul R. Challen, Diane H. Peapus, Karen A. Magnus. 1997. A niobium(V) complex with mixed O,S-donor ligands. Synthesis, structure and properties of the anion tris(2-mercapto-4-methylphenolato)niobate(V). *Polyhedron* **16**:9, 1447-1451. [Crossref]

20. Stephen A. Kubow, Kenneth J. Takeuchi, Joseph J. Grzybowski, Alan J. Jircitano, Virgil L. Goedken. 1996. Distortions from trigonal prismatic geometry for several structurally characterized clathrochelate complexes: significance of π-backbonding on clathrochelate coordination geometry. *Inorganica Chimica Acta* **241**:2, 21-30. [Crossref]

21. Douglas W. Stephan, T. Timothy Nadasdi. 1996. Early transition metal thiolates. *Coordination Chemistry Reviews* **147**, 147-208. [Crossref]

22. Wolfram Stüer, Kristin Kirschbaum, Dean M. Giolando. 1994. Homoleptische Thiolatokomplexe: Metall-Schwefel-Gerüste mit unerwarteter Struktur in den zwei- und dreikernigen TiIV-Komplexen [Ti2(SMe)9]− bzw. [Ti3(SMe)12]. *Angewandte Chemie* **106**:19, 2028-2030. [Crossref]

23. Martin Könemann, Wolfram Stüer, Kristin Kirschbaum, Dean M. Giolando. 1994. Synthesis, crystal structure and electrochemistry of bis(N,N-dimethylammonium) tris(1,2-benzenedithiolato)titanate(IV). *Polyhedron* **13**:9, 1415-1425. [Crossref]